Eur. Phys. J. Plus (2020) 135:29
https://doi.org/10.1140/epjp/s13360-019-00007-0

THE EUROPEAN PHYSICAL JOURNAL PLUS

Regular Article

Two reliable methods for solving the forced convection in a porous-saturated duct

M. S. Hashemi[1], **M. Inc**[2,a], **N. Seyfi**[1], **M. Bayram**[3]

[1] Department of Mathematics, Basic Science Faculty, University of Bonab, P.O. Box 55517-61167, Bonab, Iran
[2] Department of Mathematics, Firat University, Elazig, Turkey
[3] Department of Computer Engineering, Istanbul Gelisim University, Istanbul, Turkey

Received: 17 January 2019 / Accepted: 25 September 2019 / Published online: 9 January 2020

Abstract In this paper, the solution of nonlinear forced convection in a porous saturable duct is numerically approximated by two different approaches. The first one is a Lie group integrator based on the group $SL_2(R)$, whose calculation is far simpler and easier. The second method is reproducing kernel Hilbert space (RKHS) method which uses the Hilbert spaces in calculation. Convergence analyses for both methods were done. Effects of the porous media shaped parameter, Forchheimer number, and viscosity ratio on the solutions are discussed and illustrated by the proposed methods. The numerical experimentsshowed that the $SL_2(R)$-shooting method and RKHS method are suitable for solving the forced convection in a porous-saturated duct with high accuracy and efficiency.

1 Introduction

In most of the mechanical systems and other branches of science and engineering, differential equation plays a significant role. In most of these models, partial differential equations, fractional differential equations, and other types of differential equations can be reduced by transformations such as similarity variables or reduction methods into ordinary differential equations with initial or boundary conditions. Therefore, investigating the obtained differential equations has an important role in the explanation of phenomena. It is well known that analytical methods are not applicable for most of the ordinary differential equations. Hence, we have to apply approximation theory to solve them.

In this paper, we use a Lie group-based method [1–9] and RKHS method [10–18], which have recently become of great interest for scholars.

The major difference between Lie group-based method and the traditional numerical methods is that those schemes are all formulated directly in the usual Euclidean space R^n; none of them are considered in the Minkowski space. One of the benefits of Lie group-based method in the augmented Minkowski space is that the resulting schemes can avoid the spurious solutions and ghost fixed points. Moreover, the RKHS method is in the class of meshless methods. The main difference between the meshfree and well-known finite-element method (FEM) is the shape functions used to approximate the trial and test functions

[a] e-mail: minc@firat.edu.tr

of discretization. The key is using overlapping domains in meshfree methods, which gives more support nodes for each point, allowing a richer approximation and avoiding any artificial discontinuity in the field.

Let us consider the dimensionless form of the Brinkman–Forchheimer momentum equation with the symmetry boundary conditions [19–21] as:

$$\frac{\mathrm{d}^2 u}{\mathrm{d}\xi^2} - s^2 u - F s u^2 + \frac{1}{m} = 0;\quad BC's \rightarrow \begin{cases} \frac{\mathrm{d}u}{\mathrm{d}\xi} = 0 \text{ at } \xi = 0 \\ u = 0 \text{ at } \xi = 1, \end{cases} \tag{1.1}$$

where

$$s = \frac{1}{\sqrt{m\mathrm{Da}}} \tag{1.2}$$

is well known as the porous media shape parameter. The values

$$m = \frac{\mu_{\mathrm{eff}}}{\mu},\ \mathrm{Da} = \frac{K}{H^2},\ F = \frac{C_{\mathrm{F}} \rho G H^3}{\mu_{\mathrm{eff}} \mu} \tag{1.3}$$

are the viscosity ratio, the Darcy number, and the Forchheimer number, respectively. Moreover, μ_{eff} is an effective viscosity, μ is the fluid viscosity, K is the permeability, H is the half channel distance, ρ is the fluid density, C_{F} is the inertial coefficient, and G is the negative applied pressure gradient.

Three kinds of Poiseuille–Couette combinations, along with the central models governing flow through porous media, are considered by Awartani et al. [19]. Hooman [20] considered the forced convection through a porous medium bounded by two isoflux parallel plates using the asymptotic expansion method. Abbasbandy et al. [21] have considered the forced convection in a porous-saturated duct.

2 A Lie group $SL_2(R)$-shooting method

In the part of constructing a Lie group $SL_2(R)$-shooting method, it is supposed that $u(\xi) > -\infty$, and there exists $\kappa \in R\backslash\{0\}$, such that

$$\theta(\xi) = u(\xi) + \kappa > 0,\quad \xi \in [\xi_0, \xi_f] = [0, 1]. \tag{2.4}$$

Then, Eq. (1.1) becomes:

$$\frac{\mathrm{d}^2 \theta}{\mathrm{d}\xi^2} - s^2(\theta - \kappa) - F s(\theta - \kappa)^2 + \frac{1}{m} = 0;\quad BC's \rightarrow \begin{cases} \frac{\mathrm{d}\theta}{\mathrm{d}\xi} = 0 \text{ at } \xi = 0 \\ \theta = \kappa \text{ at } \xi = 1 \end{cases} \tag{2.5}$$

Let $\theta_1(\xi) = \theta(\xi)$ and $\theta_2(\xi) = \theta'(\xi)$. Equivalent system of Eq. (2.5) can be written as:

$$\begin{cases} \dfrac{\mathrm{d}\theta_1(\xi)}{\mathrm{d}\xi} = \theta_2(\xi), \\ \dfrac{\mathrm{d}\theta_2(\xi)}{\mathrm{d}\xi} = s^2(\theta_1(\xi) - \kappa) + F s(\theta_1(\xi) - \kappa)^2 - \dfrac{1}{m}, \end{cases} \quad \theta_1(1) = \theta_1^f = \kappa,\ \theta_2(0) = \theta_2^0 = 0, \tag{2.6}$$

or equivalently:

$$\frac{\mathrm{d}}{\mathrm{d}\xi} \begin{pmatrix} \theta_1(\xi) \\ \theta_2(\xi) \end{pmatrix} = \begin{pmatrix} 0 & 1 \\ \varpi(\xi, \theta_1) & 0 \end{pmatrix} \begin{pmatrix} \theta_1(\xi) \\ \theta_2(\xi) \end{pmatrix}, \tag{2.7}$$

where

$$\varpi(\xi,\theta_1) := \frac{s^2(\theta_1(\xi)-\kappa)+Fs(\theta_1(\xi)-\kappa)^2}{\theta_1(\xi)} - \frac{1}{m\theta_1(\xi)}.$$

Clearly, $\varpi(\xi,\theta_1)$ is well defined, because $\theta_1(\xi) > 0$. In this paper, we can find an explicit form of the Lie group $SL_2(R)$ as:

$$\frac{\mathrm{d}}{\mathrm{d}\xi}\mathbf{G} = \mathcal{A}\mathbf{G}, \quad \mathbf{G}(0) = I_{2\times 2}, \tag{2.8}$$

with $\det(\mathbf{G}) = 1$ and

$$\mathcal{A} = \begin{pmatrix} 0 & 1 \\ \varpi & 0 \end{pmatrix}.$$

This is not an easy task because of the appearance of nonlinear term $\varpi(\xi,\theta_1)$ in Eq. (2.7). Now, we like to suppose an iterative method to solve Eq. (2.7):

$$\Theta_{n+1} = \mathbf{G}(n)\Theta_n, \tag{2.9}$$

where $\mathbf{G}(n)$ is an element of $SL_2(R)$ and $\Theta_n := \Theta|_{\xi=\xi_n}$. Desired value $\Theta(\xi)$ can be obtained by solving Eq. (2.7) using Eq. (2.9) and initial value $\Theta(0) = \Theta_0$. Let $N = \frac{1}{\Delta\xi}$[1] be the number of GPS iterations:

$$\Theta_{n+1} = \Theta_n + \frac{(\alpha_n - 1)\mathcal{F}_n.\Theta_n + \beta_n\|\Theta_n\|\|\mathcal{F}_n\|}{\|\mathcal{F}_n\|^2}\mathcal{F}_n,$$

where

$$\alpha_n = \cosh\left(\frac{\Delta\xi\|\mathcal{F}_n\|}{\Theta_n}\right), \quad \beta_n = \sinh\left(\frac{\Delta\xi\|\mathcal{F}_n\|}{\Theta_n}\right).$$

This method is an explicit integrator of initial value problem:

$$\begin{cases} \Theta' = \mathcal{F}(\xi,\Theta), \\ \Theta(0) = \Theta_0. \end{cases} \tag{2.10}$$

Moreover:

$$\Theta_f = \mathbf{G}_N(\Delta\xi)\cdots\mathbf{G}_1(\Delta\xi)\Theta_0, \tag{2.11}$$

gives the value of $\theta(1)$ as θ_f. Let us suppose $\mathbf{G}(\Delta\xi) := \mathbf{G}_N(\Delta\xi)\cdots\mathbf{G}_1(\Delta\xi)$, and then, one can write a one-step Lie group transformation from Θ_0 to Θ_f as:

$$\Theta_f = \mathbf{G}\Theta_0, \quad \mathbf{G} \in SL_2(R). \tag{2.12}$$

It can be concluded from the exponential map in manifolds and from integration of (2.8), that:

$$\mathbf{G}(\xi) = exp\left(\int_0^\xi \mathcal{A}(\sigma)d\sigma\right). \tag{2.13}$$

If we let

$$\begin{aligned} \tilde{\xi} &= r\xi_0 + (1-r)\xi_f = 1-r, \\ \tilde{\theta}_1 &= r\theta_1^0 + (1-r)\theta_1^f = r\theta_1^0 + \kappa(1-r), \\ \tilde{\theta}_2 &= r\theta_2^0 + (1-r)\theta_2^f = (1-r)\theta_2^f, \end{aligned}$$

[1] $\Delta\xi$ is step-size in ξ direction.

where $r \in [0, 1]$ to be determined later, we get:

$$\mathbf{G}(r) = \exp(\mathcal{A}(\tilde{\xi}, \tilde{\theta}_1)), \tag{2.14}$$

with

$$\mathcal{A}(\tilde{\xi}, \tilde{\theta}_1) =: \begin{pmatrix} 0 & 1 \\ \varpi & 0 \end{pmatrix} = \begin{pmatrix} 0 & 1 \\ \varpi(\tilde{\xi}, \tilde{\theta}_1) & 0 \end{pmatrix}, \tag{2.15}$$

and

$$\varpi = \varpi(\tilde{\xi}, \tilde{\theta}_1) = \frac{s^2(\tilde{\theta}_1 - \kappa) + Fs(\tilde{\theta}_1 - \kappa)^2}{\tilde{\theta}_1} - \frac{1}{m\tilde{\theta}_1}.$$

In the current work, $\theta_1^f = \kappa,\ \theta_2^0 = 0$ are known, and $\theta_2^f,\ \theta_1^0$ are unknown boundaries. We will try to determine θ_1^0 as a missing initial value. The values for $\mathbf{G}$ in Eq. (2.14) generated from $\mathcal{A} \in SL_2(R)$ have the following explicit forms:

$$\mathbf{G}(r) = \begin{pmatrix} \cos(\sqrt{-\varpi}) & -\frac{\sin(\sqrt{-\varpi})}{\sqrt{-\varpi}} \\ -\sqrt{-\varpi}\ \sin(\sqrt{-\varpi}) & \cos(\sqrt{-\varpi}) \end{pmatrix}, \text{ if } \varpi < 0, \tag{2.16}$$

$$\mathbf{G}(r) = \begin{pmatrix} \cosh(\sqrt{\varpi}) & \frac{\sinh(\sqrt{\varpi})}{\sqrt{\varpi}} \\ \sqrt{\varpi}\ \sinh(\sqrt{\varpi}) & \cosh(\sqrt{\varpi}) \end{pmatrix}, \text{ if } \varpi > 0, \tag{2.17}$$

$$\mathbf{G}(r) = \begin{pmatrix} 1 & 1 \\ 0 & 1 \end{pmatrix}, \text{ if } \varpi = 0. \tag{2.18}$$

From Eqs. (2.12) and (2.16)–(2.18), we obtain:

$$\begin{pmatrix} \theta_1^f \\ \theta_2^f \end{pmatrix} = \begin{pmatrix} \cos(\sqrt{-\varpi}) & -\frac{\sin(\sqrt{-\varpi})}{\sqrt{-\varpi}} \\ -\sqrt{-\varpi}\ \sin(\sqrt{-\varpi}) & \cos(\sqrt{-\varpi}) \end{pmatrix} \begin{pmatrix} \theta_1^0 \\ \theta_2^0 \end{pmatrix}, \text{ if } \varpi < 0, \tag{2.19}$$

$$\begin{pmatrix} \theta_1^f \\ \theta_2^f \end{pmatrix} = \begin{pmatrix} \cosh(\sqrt{\varpi}) & \frac{\sinh(\sqrt{\varpi})}{\sqrt{\varpi}} \\ \sqrt{\varpi}\ \sinh(\sqrt{\varpi}) & \cosh(\sqrt{\varpi}) \end{pmatrix} \begin{pmatrix} \theta_1^0 \\ \theta_2^0 \end{pmatrix}, \text{ if } \varpi > 0, \tag{2.20}$$

$$\begin{pmatrix} \theta_1^f \\ \theta_2^f \end{pmatrix} = \begin{pmatrix} 1 & 1 \\ 0 & 1 \end{pmatrix} \begin{pmatrix} \theta_1^0 \\ \theta_2^0 \end{pmatrix}, \text{ if } \varpi = 0. \tag{2.21}$$

Thus, for a given r and from $\theta_1^f = \kappa, \theta_2^0 = 0$, we obtain:

$$\begin{cases} \theta_1^f = \cos(\sqrt{-\varpi})\theta_1^0 - \frac{\sin(\sqrt{-\varpi})}{\sqrt{-\varpi}}\theta_2^0, \\ \theta_2^f = -\sqrt{-\varpi}\ \sin(\sqrt{-\varpi})\theta_1^0 + \cos(\sqrt{-\varpi})\theta_2^0, \end{cases} \Rightarrow \begin{cases} \theta_1^0 = \kappa \sec(\sqrt{-\varpi}), \\ \theta_2^f = -\kappa\sqrt{-\varpi}\tan(\sqrt{-\varpi}), \end{cases} \tag{2.22}$$

when $\varpi < 0$, and

$$\begin{cases} \theta_1^f = \cosh(\sqrt{\varpi})\theta_1^0 + \frac{\sinh(\sqrt{\varpi})}{\sqrt{\varpi}}\theta_2^0, \\ \theta_2^f = \sqrt{\varpi}\ \sinh(\sqrt{\varpi})\theta_1^0 + \cosh(\sqrt{\varpi})\theta_2^0, \end{cases} \Rightarrow \begin{cases} \theta_1^0 = \kappa\,\mathrm{sech}(\sqrt{\varpi}), \\ \theta_2^f = \kappa\sqrt{\varpi}\tanh(\sqrt{\varpi}), \end{cases} \tag{2.23}$$

when $\varpi > 0$. Finally, for $\varpi = 0$, we get:

$$\begin{cases} \theta_1^0 = \kappa, \\ \theta_2^f = 0. \end{cases} \tag{2.24}$$

Now, we summarize our proposed method as the following algorithm:
(i) Take an arbitrary $0 \le r \le 1$ and initial guesses θ_1^0 and θ_2^f, respectively.
(ii) Compute

$$\begin{cases} \tilde{\xi} = r\xi_0 + (1-r)\xi_f = 1-r, \\ \tilde{\theta}_1 = r\theta_1^0 + (1-r)\theta_1^f = r\theta_1^0 + \kappa(1-r), \\ \tilde{\theta}_2 = r\theta_2^0 + (1-r)\theta_2^f = (1-r)\theta_2^f. \end{cases}$$

(iii) Find the following values for $n = 1, 2, \ldots$:

$$\tilde{\theta}_1(n) = r\theta_1^0(n-1) + \kappa(1-r),$$
$$\tilde{\theta}_2(n) = (1-r)\theta_2^f(n-1),$$
$$\varpi(n) = \frac{s^2(\tilde{\theta}_1(n)-\kappa) + Fs(\tilde{\theta}_1(n)-\kappa)^2}{\tilde{\theta}_1(n)} - \frac{1}{m\tilde{\theta}_1(n)},$$
$$\begin{cases} \theta_1^0(n) = \kappa\ \sec(\sqrt{-\varpi(n)}), \\ \theta_2^f(n) = -\kappa\sqrt{-\varpi(n)}\tan(\sqrt{-\varpi(n)}), \end{cases} \quad \text{if } \varpi(n) < 0,$$
$$\begin{cases} \theta_1^0(n) = \kappa\ \text{sech}(\sqrt{\varpi(n)}), \\ \theta_2^f(n) = \kappa\sqrt{\varpi(n)}\tanh(\sqrt{\varpi(n)}), \end{cases} \quad \text{if } \varpi(n) > 0,$$
$$\begin{cases} \theta_1^0(n) = \kappa, \\ \theta_2^f(n) = 0, \end{cases} \quad \text{if } \varpi(n) = 0.$$

If

$$\sqrt{\left(\theta_1^0(n) - \theta_1^0(n-1)\right)^2 + \left(\theta_2^f(n) - \theta_2^f(n-1)\right)^2} \le \epsilon \tag{2.25}$$

holds, then stop; otherwise return to (iii).

For a trial r, we do this algorithm, and then, we minimize the problem:

$$\min_{r\in[0,1]} \left|\theta_1^f - \kappa\right|, \tag{2.26}$$

to find the best r.

3 Reproducing kernel functions

In this section, we describe the RKHS method and its preliminaries. We give some reproducing kernel functions.

Definition 3.1 Let $P \neq \emptyset$. A function $Z : P \times P \to \mathbb{C}$ is called a *reproducing kernel function* of the Hilbert space H if and only if:

(a) $Z(\cdot, x) \in H$ for all $x \in P$.
(b) $\langle \varrho, Z(\cdot, x)\rangle = \varrho(x)$ for all $x \in P$ and all $\varrho \in H$.

Let us denote AC as the space of absolutely continuous functions.

Definition 3.2 $\mathcal{W}_2^1[0, 1]$ is given as:

$$\mathcal{W}_2^1[0,1] = \{u : u \in AC[0,1]\ \ and\ \ u' \in L^2[0,1]\},$$

with

$$\langle u, g\rangle_{\mathcal{W}_2^1} = \int_0^1 \left[u(\xi)g(\xi) + u'(\xi)g'(\xi)\right]\mathrm{d}\xi, \quad u, g \in \mathcal{W}_2^1[0,1] \tag{3.27}$$

and

$$\|u\|_{\mathcal{W}_2^1} = \sqrt{\langle u, u\rangle_{\mathcal{W}_2^1}}, \quad u \in \mathcal{W}_2^1[0,1], \tag{3.28}$$

as the inner product and the norm in $\mathcal{W}_2^1[0,1]$, respectively. Reproducing kernel function $T_\xi(u)$ of $\mathcal{W}_2^1[0,1]$ is given by:

$$T_\xi(u)= \frac{1}{2\sinh(1)}\left[\cosh(\xi+u-1)+\cosh(|\xi-u|-1)\right]. \tag{3.29}$$

Definition 3.3 The space ${}^o\mathcal{W}_2^3[0,1]$ is given by:

$${}^o\mathcal{W}_2^3[0,1] = \{u \in AC[0,1]:\ u', u'' \in AC[0,1],\ u^{(3)} \in L^2[0,1],\ u'(0) = 0 = u(1)\}.$$

$$\langle u, v\rangle_{{}^o\mathcal{W}_2^3[0,1]} = u(0)v(0)+u'(0)v'(0)+u(1)v(1)+\int_0^1 u^{(3)}(\xi)v^{(3)}(\xi)\mathrm{d}\xi,\ \ u, v\in {}^o\mathcal{W}_2^3[0,1],$$

and

$$\|u\|_{{}^o\mathcal{W}_2^3[0,1]} = \sqrt{\langle u, u\rangle_{{}^o\mathcal{W}_2^3[0,1]}}, \quad u \in^o \mathcal{W}_2^3[0,1],$$

are the inner product and the norm in ${}^o\mathcal{W}_2^3[0,1]$, respectively.

Theorem 3.1 *Reproducing kernel function $R_y(\xi)$ of ${}^o\mathcal{W}_2^3[0,1]$ is given as:*

$$\mathcal{R}_y(\xi) = \begin{cases} -\frac{1}{120}\xi^5y^2 + \frac{1}{120}\xi^5 + \frac{1}{24}\xi^4y^2 - \frac{1}{24}\xi^4y + 1 - \frac{1}{12}\xi^2y^3 \\ -\frac{1}{120}\xi^2y^5 + \frac{1}{24}\xi^2y^4 + \frac{21}{20}\xi^2y^2 - \xi^2 - y^2, \quad 0 \le \xi \le y \le 1, \\ -\frac{1}{120}\xi^2y^5 + \frac{1}{120}y^5 + \frac{1}{24}\xi^2y^4 - \frac{1}{24}y^4\xi + 1 - \frac{1}{12}\xi^3y^2 \\ -\frac{1}{120}\xi^5y^2 + \frac{1}{24}\xi^4y^2 + \frac{21}{20}\xi^2y^2 - \xi^2 - y^2, \quad 0 \le y < \xi \le 1. \end{cases} \tag{3.30}$$

Proof First, let us suppose:

$$\mathcal{R}_y(\xi) = \begin{cases} \sum_{i=1}^6 c_i(y)\xi^{i-1}, & 0 \le \xi \le y \le 1, \\ \sum_{i=1}^6 d_i(y)\xi^{i-1}, & 0 \le y < \xi \le 1. \end{cases} \tag{3.31}$$

Then, from $u \in {}^0\mathcal{W}_2^3[0,1]$, we get:

$$\begin{aligned}\left\langle u, \mathcal{R}_y(\xi)\right\rangle_{{}^o\mathcal{W}_2^3[0,1]} &= u(0)\mathcal{R}_y(0) + u'(0)\mathcal{R}_y'(0) + u(1)\mathcal{R}_y(1) + \int_0^1 u^{(3)}(\xi)\frac{\partial^3\mathcal{R}_y(\xi)}{\partial\xi^3}\mathrm{d}\xi \\ &= u(0)\mathcal{R}_y(0) + u''(1)\frac{\partial^3\mathcal{R}_y(1)}{\partial\xi^3} - u''(0)\frac{\partial^3\mathcal{R}_y(0)}{\partial\xi^3} - u'(1)\frac{\partial^4\mathcal{R}_y(1)}{\partial\xi^4} \\ &\quad +u'(0)\frac{\partial^4\mathcal{R}_y(0)}{\partial\xi^4} + u(1)\frac{\partial^5\mathcal{R}_y(1)}{\partial\xi^5} \\ &\quad -u(0)\frac{\partial^5\mathcal{R}_y(0)}{\partial\xi^5} - \int_0^1 u(\xi)\frac{\partial^6\mathcal{R}_y(\xi)}{\partial\xi^6}\mathrm{d}\xi. \end{aligned} \tag{3.32}$$

Substituting (3.31) in (3.32) and solving the coefficients as equations, we get the reproducing kernel function as:

$$\mathcal{R}_y(\xi) = \begin{cases} -\frac{1}{120}\xi^5 y^2 + \frac{1}{120}\xi^5 + \frac{1}{24}\xi^4 y^2 - \frac{1}{24}\xi^4 y + 1 - \frac{1}{12}\xi^2 y^3 \\ -\frac{1}{120}\xi^2 y^5 + \frac{1}{24}\xi^2 y^4 + \frac{21}{20}\xi^2 y^2 - \xi^2 - y^2, \quad 0 \le \xi \le y \le 1, \\ -\frac{1}{120}\xi^2 y^5 + \frac{1}{120} y^5 + \frac{1}{24}\xi^2 y^4 - \frac{1}{24} y^4 \xi + 1 - \frac{1}{12}\xi^3 y^2 \\ -\frac{1}{120}\xi^5 y^2 + \frac{1}{24}\xi^4 y^2 + \frac{21}{20}\xi^2 y^2 - \xi^2 - y^2, \quad 0 \le y < \xi \le 1. \end{cases} \tag{3.33}$$

This completes the proof. □

3.1 Solutions in ${}^o\mathcal{W}_2^3[0, 1]$

The solution of Eq. (1.1) is considered in the reproducing kernel space ${}^o\mathcal{W}_2^3[0, 1]$ in this section. On defining the linear operator:

$$\mathcal{L} : \ {}^o\mathcal{W}_2^3[0, 1] \to \mathcal{W}_2^1[0, 1]$$

as

$$\mathcal{L}u(\xi) = u''(\xi) \tag{3.34}$$

problem (1.1) converts the form:

$$\begin{cases} \mathcal{L}u = \mathfrak{f}(\xi, u), \quad \xi \in [0, 1], \\ u'(0) = 0 = u(1), \end{cases} \tag{3.35}$$

with

$$\mathfrak{f}(\xi, u) = s^2 u + F s u^2 - \frac{1}{m}. \tag{3.36}$$

Theorem 3.2 *The operator $\mathcal{L}$ given by (3.34) is a bounded linear operator.*

Proof First, we show that $\|\mathcal{L}u\|^2_{\mathcal{W}_2^1} \le \mathcal{M} \|u\|^2_{{}^o\mathcal{W}_2^3}$, with $\mathcal{M} > 0$. From (3.27) and (3.28), we get:

$$\|\mathcal{L}u\|^2_{\mathcal{W}_2^1} = \langle \mathcal{L}u, \mathcal{L}u \rangle_{\mathcal{W}_2^1} = \int_0^1 [(\mathcal{L}u)(\xi)^2 + (\mathcal{L}u)'(\xi)^2] \mathrm{d}\xi.$$

Moreover, reproducing properties:

$$u(\xi) = \left\langle u(\cdot), \mathcal{R}_y(\xi)(\cdot) \right\rangle_{{}^o\mathcal{W}_2^3},$$

and

$$\mathcal{L}u(\xi) = \left\langle u(\cdot), \mathcal{L}\mathcal{R}_y(\xi)(\cdot) \right\rangle_{{}^o\mathcal{W}_2^3}$$

concludes

$$|\mathcal{L}u(\xi)| \le \|u\|_{{}^o\mathcal{W}_2^3} \left\|\mathcal{L}\mathcal{R}_y(\xi)\right\|_{{}^o\mathcal{W}_2^3} = \mathcal{M}_1 \|u\|_{{}^o\mathcal{W}_2^3},$$

where $\mathcal{M}_1 > 0$. Thus, we get:

$$\int_0^1 [(\mathcal{L}u)(\xi)]^2 \mathrm{d}\xi \le \mathcal{M}_1^2 \|u\|^2_{{}^o\mathcal{W}_2^3}.$$

Also, from

$$(\mathcal{L}u)'(\xi) = \left\langle u(\cdot), (\mathcal{L}\mathcal{R}_y(\xi))'(\cdot)\right\rangle_{{}^o\mathcal{W}_2^3},$$

we have:

$$\left|(\mathcal{L}u)'(\xi)\right| \leq \|u\|_{{}^o\mathcal{W}_2^3} \left\|(\mathcal{L}\mathcal{R}_y(\xi))'\right\|_{{}^o\mathcal{W}_2^3} = \mathcal{M}_2 \|u\|_{{}^o\mathcal{W}_2^3},$$

where $\mathcal{M}_2 > 0$. Thus, we get:

$$\left[(\mathcal{L}u)'(\xi)\right]^2 \leq \mathcal{M}_2^2 \|u\|^2_{{}^o\mathcal{W}_2^3},$$

and

$$\int_0^1 \left[(\mathcal{L}u)'(\xi)\right]^2 \mathrm{d}\xi \leq \mathcal{M}_2^2 \|u\|^2_{{}^o\mathcal{W}_2^3},$$

is

$$\|\mathcal{L}u\|^2_{\mathcal{W}_2^1} = \int_0^1 ([(\mathcal{L}u)(\xi)]^2 + \left[(\mathcal{L}u)'(\xi)\right]^2)\mathrm{d}\xi \leq \left(\mathcal{M}_1^2 + \mathcal{M}_2^2\right) \|u\|^2_{{}^o\mathcal{W}_2^3} = \mathcal{M} \|u\|^2_{{}^o\mathcal{W}_2^3},$$

where $\mathcal{M} = \mathcal{M}_1^2 + \mathcal{M}_2^2 > 0$. □

3.2 Structure of the solution and the main results

Obviously, the defined operator from (3.34) as $\mathcal{L} : {}^o\mathcal{W}_2^3[0, 1] \to \mathcal{W}_2^1[0, 1]$ is a bounded linear operator. Put $\varphi_i(\xi) = T_{\xi_i}(\xi)$ and $\psi_i(\xi) = \mathcal{L}^*\varphi_i(\xi)$, where $\mathcal{L}^*$ is conjugate operator of $\mathcal{L}$. The orthonormal system $\{\hat{\psi}_i(\xi)\}_1^\infty \subseteq {}^0\mathcal{W}_2^3[0, 1]$ can be derived from the well-known Gram-Schmidt orthogonalization process of $\{\psi_i(\xi)\}_1^\infty$:

$$\hat{\psi}_i(\xi) = \sum_{k=1}^{i} \beta_{ik}\psi_k(\xi), \ \ (\beta_{ii} > 0, i = 1, 2, \ldots). \tag{3.37}$$

Theorem 3.3 *Let us suppose* $\{\xi_i\}_{i=1}^\infty$ *be dense in* $[0, 1]$ *and* $\psi_i(\xi) = \mathcal{L}_y R_\xi(y)|_{y=\xi_i}$. *Then, the sequence* $\{\psi_i(\xi)\}_{i=1}^\infty$ *is a complete system in* ${}^0\mathcal{W}_2^3[0, 1]$.

Proof Let us construct an explicit form of $\psi_i(\xi)$ as follows:

$$\psi_i(\xi) = (\mathcal{L}^*\varphi_i)(\xi) = \left\langle(\mathcal{L}^*\varphi_i)(y), \mathcal{R}_\xi(y)\right\rangle = \left\langle(\varphi_i)(y), \mathcal{L}_y\mathcal{R}_\xi(y)\right\rangle = \mathcal{L}_y\mathcal{R}_\xi(y)|_{y=\xi_i};$$

obviously, $\psi_i(\xi) \in {}^0\mathcal{W}_2^3[0, 1]$. For each fixed $u(\xi) \in {}^0\mathcal{W}_2^3[0, 1]$, let $\langle u(\xi), \psi_i(\xi)\rangle = 0$, $(i = 1, 2, \ldots)$, which means that:

$$\left\langle u(\xi), (\mathcal{L}^*\varphi_i)(\xi)\right\rangle = \langle \mathcal{L}u(\cdot), \varphi_i(\cdot)\rangle = (\mathcal{L}u)(\xi_i) = 0.$$

Note that $\{\xi_i\}_{i=1}^\infty$ is dense in $[0, 1]$; therefore, $(\mathcal{L}u)(\xi) = 0$. From the existence of $\mathcal{L}^{-1}$, it concludes that $u \equiv 0$. □

Theorem 3.4 *If* $u(\xi)$ *is the exact solution of* (3.35), *then*

$$u(\xi) = \sum_{i=1}^{\infty}\sum_{k=1}^{i} \beta_{ik}\mathfrak{f}(\xi_k, u_k)\hat{\psi}_i(\xi), \tag{3.38}$$

where $\{(\xi_i)\}_{i=1}^\infty$ *is dense in* $[0, 1]$.

Proof From the (3.37) and uniqueness of the solution of (3.35), we get:

$$\begin{aligned} u(\xi) &= \sum_{i=1}^{\infty} \left\langle u(\xi), \hat{\psi}_i(\xi) \right\rangle_{^0\mathcal{W}_2^3} \hat{\psi}_i(\xi) \\ &= \sum_{i=1}^{\infty} \sum_{k=1}^{i} \beta_{ik} \left\langle u(\xi), \psi_k(\xi) \right\rangle_{^0\mathcal{W}_2^3} \hat{\psi}_i(\xi) \\ &= \sum_{i=1}^{\infty} \sum_{k=1}^{i} \beta_{ik} \left\langle u(\xi), \mathcal{L}^*\varphi_k(\xi) \right\rangle_{^0\mathcal{W}_2^3} \hat{\psi}_i(\xi) \\ &= \sum_{i=1}^{\infty} \sum_{k=1}^{i} \beta_{ik} \left\langle \mathcal{L}u(\xi), \varphi_k(\xi) \right\rangle_{\mathcal{W}_2^1} \hat{\psi}_i(\xi) \\ &= \sum_{i=1}^{\infty} \sum_{k=1}^{i} \beta_{ik} \left\langle \mathfrak{f}(\xi, u), T_{\xi_k} \right\rangle_{\mathcal{W}_2^1} \hat{\psi}_i(\xi) = \sum_{i=1}^{\infty} \sum_{k=1}^{i} \beta_{ik} \mathfrak{f}(\xi_k, u_k) \hat{\psi}_i(\xi). \end{aligned}$$

Finite terms of (3.38) conclude the approximate solution:

$$u_n(\xi) = \sum_{i=1}^{\infty} \sum_{k=1}^{i} \beta_{ik} \mathfrak{f}(\xi_k, u_k) \hat{\psi}_i(\xi). \tag{3.39}$$

□

Lemma 3.1 *If* $\|u_n - u\|_{^0\mathcal{W}_2^3} \to 0$, $\xi_n \to \xi$, *and* $\mathfrak{f}(\xi, u)$ *is continuous w.r.t.* $\xi \in [0, 1]$, *then:*

$$\mathfrak{f}(\xi_n, u_{n-1}(\xi_n)) \to \mathfrak{f}(\xi, u(\xi)), \quad as \quad n \to \infty.$$

In the following, we present a theorem which demonstrate the structure of approximate solution. Then, the convergence analysis of approximate solution is proved.

Theorem 3.5 *Let for any fixed* $u_0(\xi) \in {}^0\mathcal{W}_2^3[0, 1]$, *we have:*

(i)

$$u_n(\xi) = \sum_{i=1}^{n} A_i \hat{\psi}_i(\xi), \tag{3.40}$$

$$A_i = \sum_{k=1}^{i} \beta_{ik} \mathfrak{f}(\xi_k, u_{k-1}(\xi_k)). \tag{3.41}$$

(ii) $\|u_n\|_{^0\mathcal{W}_2^3}$ *is bounded.*
(iii) $\{\xi_i\}_{i=1}^{\infty}$ *is dense in* $[0, 1]$.
(iv) $\mathfrak{f}(\xi, u) \in \mathcal{W}_2^1[0, 1]$ *for any* $u(\xi) \in {}^0\mathcal{W}_2^3[0, 1]$. *Then, the approximate solution* $u_n(\xi)$ *converges to the exact solution of* (3.38) *in* ${}^0\mathcal{W}_2^3$ *and*

$$u(\xi) = \sum_{i=1}^{\infty} A_i \hat{\psi}_i(\xi).$$

Proof First, we prove the convergence of $u_n(\xi)$. From (3.40), we have:

$$u_{n+1}(\xi) = u_n(\xi) + A_{n+1}\hat{\psi}_{n+1}(\xi) \tag{3.42}$$

from the orthonormality of $\{\hat{\psi}_i\}_{i=1}^{\infty}$, it follows that:

$$\|u_{n+1}\|^2 = \|u_{n+1}\|^2 + A_{n+1}^2 = \|u_{n-1}\|^2 + A_n^2 + A_{n+1}^2 = \cdots = \sum_{i=1}^{n+1} A_i^2 \tag{3.43}$$

and from boundedness of$\|u_n\|_{{}^0\mathcal{W}_2^3}$, we obtain:

$$\sum_{i=1}^{\infty} A_i^2 < \infty,$$

i.e.,

$$\{A_i\} \in l^2 \quad (i = 1, 2, \ldots).$$

Let $m > n$, in view of $(u_m - u_{m-1}) \perp (u_{m-1} - u_{m-2}) \perp \cdots \perp (u_{n+1} - u_n)$, we get:

$$\begin{aligned} \|u_m - u_n\|^2_{{}^0\mathcal{W}_2^3} &= \|u_m - u_{m-1} + u_{m-1} - u_{m-2} + \cdots + u_{n+1} - u_n\|^2_{{}^0\mathcal{W}_2^3} \\ &\le \|u_m - u_{m-1}\|^2_{{}^0\mathcal{W}_2^3} + \cdots + \|u_{n+1} - u_n\|^2_{{}^0\mathcal{W}_2^3} \\ &= \sum_{i=n+1}^{m} A_i^2 \to 0, \quad m, n \to \infty. \end{aligned}$$

Considering the completeness of ${}^0\mathcal{W}_2^3[0, 1]$, there exists $u(\xi) \in {}^0\mathcal{W}_2^3[0, 1]$, such that:

$$u_n(\xi) \to u(\xi) \quad as\ n \to \infty.$$

(ii) Now, we show $u(\xi)$ is the solution of (3.35). Taking limits in (3.40), we get:

$$u(\xi) = \sum_{i=1}^{\infty} A_i \hat{\psi}_i(\xi).$$

Since

$$\begin{aligned} (\mathcal{L}u)(\xi_j) &= \sum_{i=1}^{\infty} A_i \left\langle \mathcal{L}\hat{\psi}_i(\xi), \varphi_i(\xi) \right\rangle_{\mathcal{W}_2^1} \\ &= \sum_{i=1}^{\infty} A_i \left\langle \hat{\psi}_i(\xi), \mathcal{L}^*\varphi_i(\xi) \right\rangle_{{}^0\mathcal{W}_2^3} = \sum_{i=1}^{\infty} A_i \left\langle \hat{\psi}_i(\xi), \psi_j(\xi) \right\rangle_{{}^0\mathcal{W}_2^3}, \end{aligned}$$

it follows that:

$$\begin{aligned} \sum_{j=1}^{n} \beta_{nj} (\mathcal{L}u)(\xi_j) &= \sum_{i=1}^{\infty} A_i \left\langle \hat{\psi}_i(\xi), \sum_{j=1}^{n} \beta_{nj} \psi_i(\xi) \right\rangle_{{}^0\mathcal{W}_2^3} \\ &= \sum_{i=1}^{\infty} A_i \left\langle \hat{\psi}_i(\xi), \hat{\psi}_n(\xi) \right\rangle_{{}^0\mathcal{W}_2^3} = A_n. \end{aligned}$$

If $n = 1$, then

$$\mathcal{L}u(\xi_1) = \mathfrak{f}(\xi_1, u_0(\xi_1)). \tag{3.44}$$

If $n = 2$, then

$$\beta_{21}(\mathcal{L}u)(\xi_1) + \beta_{22}(\mathcal{L}u)(\xi_2) = \beta_{21}\mathfrak{f}(\xi_1, u_0(\xi_1)) + \beta_{22}\mathfrak{f}(\xi_2, u_1(\xi_2)). \tag{3.45}$$

From (3.44) and (3.45), it is obvious that:

$$(\mathcal{L}u)(\xi_2) = \mathfrak{f}(\xi_2, u_1(\xi_2)).$$

Moreover, by induction, we conclude:

$$(\mathcal{L}u)(\xi_j) = \mathfrak{f}(\xi_j, u_{j-1}(\xi_j)). \tag{3.46}$$

From $\overline{\{\xi_i\}_1^\infty} = [0, 1]$, it can be concluded that for any $y \in [0, 1]$, there exists subsequence $\{\xi_{n_j}\}_1^\infty \subseteq \{\xi_i\}_1^\infty$, such that $lim_{j\to\infty}\xi_{n_j} = y$. Therefore, convergence of $u_n(\xi)$ and Lemma 4.3 yields:

$$(\mathcal{L}u)(y) = \mathfrak{f}(y, u(y)),$$

so $u(\xi)$ is the solution of (3.35) given by:

$$u(\xi) = \sum_{i=1}^{\infty} A_i\hat{\psi}_i,$$

where A_i was given by (3.41). □

Theorem 3.6 *If* $u \in {}^0\mathcal{W}_2^3[0, 1]$, *then*

$$\|u_n - u\|_{^0\mathcal{W}_2^3} \to 0, \quad n \to \infty.$$

Moreover, the sequence $\|u_n - u\|_{^0\mathcal{W}_2^3}$ *is monotonically decreasing in* n.

Proof From (3.38) and (3.39), it follows that

$$\|u_n - u\|_{^0\mathcal{W}_2^3} = \left\| \sum_{i=n+1}^{\infty} \sum_{k=1}^{i} \beta_{ik}\mathfrak{f}(\xi_k, u_k)\hat{\psi}_i \right\|_{^0\mathcal{W}_2^3}.$$

Thus:

$$\|u_n - u\|_{^0\mathcal{W}_2^3} \to 0, \quad n \to \infty.$$

In addition:

$$\|u_n - u\|^2_{^0\mathcal{W}_2^3} = \left\| \sum_{i=n+1}^{\infty} \sum_{k=1}^{i} \beta_{ik}\mathfrak{f}(\xi_k, u_k)\hat{\psi}_i \right\|^2_{^0\mathcal{W}_2^3}$$
$$= \sum_{i=n+1}^{\infty} \left(\sum_{k=1}^{i} \beta_{ik}\mathfrak{f}(\xi_k, u_k)\hat{\psi}_i \right)^2.$$

□

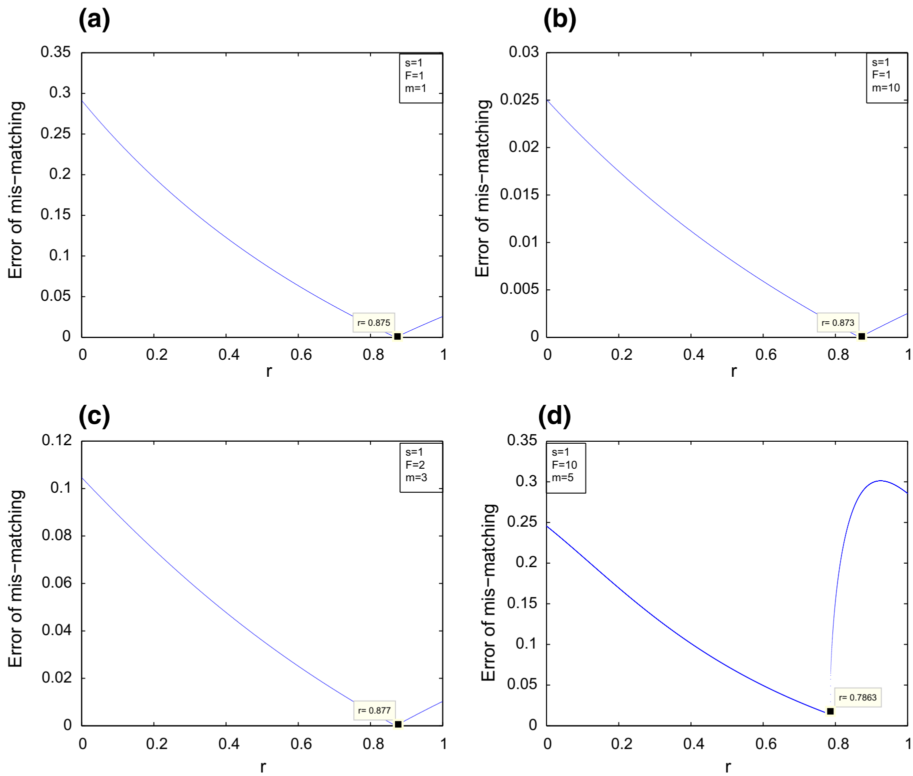

Fig. 1 Plots of mismatching errors in $SL_2(R)$-shooting method for some values of m, s and F

4 Results

When Eq. (1.1) is subjected to the Dirichlet boundary values at the boundaries of the interval $[\xi_0, \xi_f] = [0, 1]$, we have boundary value problems (BVPs). The stepping technique developed for integrating the initial value problem (IVP) needs both the initial conditions $u_1(0) = u(0)$ and $u_2(0) = u'(0)$ for the second-order ODEs. Converting Eq. (1.1) to Eq. (2.5) and starting from the initial guesses of $\theta_1(0) = \theta(0)$ and $\theta_2(0) = \theta'(0)$, we approximately solve Eq. (2.5) by GPS from $\xi = 0$ to $\xi = 1$.
In this study, the step-size $\Delta\xi = 0.01$ is used in the GPS. Taking the different investigated cases for parameters of Eq. (2.5), we assume that the starting guesses for θ_1^0 and θ_2^f are equal to unity. Moreover, the convergence criterion utilized in the current developed $SL_2(R)$-shooting method is $\epsilon = 10^{-12}$.

The choice of $r \in [0, 1]$ in our method plays a critical role in finding the approximate value of $\theta(0)$. In Fig. 1a–d, we plotted some mismatching errors for some values of F, s and m. Best choices of $r = 0.875$, $r = 0.873$, $r = 0.877$, and $r = 0.7863$ are observable from Fig. 1a–d.

From Table 1, when $F = m = 1$ and the porous media shaped parameter s is varying from 0 to 5, we can see that the maximum error of finding the initial value by the $SL_2(R)$-shooting method is about $10^{-8} \sim 10^{-10}$. In the present paper, we compare our results with Wolfram Mathematica 9 software results. This software uses the ordinary shooting method to find

Table 1 Obtained values and absolute errors of $u(0)$ and $u'(1)$ with $SL_2(R)$ method, when $F = m = 1$ and s is varying

s	$u(0)$–$SL_2(R)$	Error of $u(0)$	$u'(1)$–$SL_2(R)$	Error of $u'(1)$
0.0	0.499999997	3.0×10^{-9}	– 0.999999998	2.0×10^{-9}
0.5	0.422685396	2.6×10^{-9}	– 0.880643127	2.4×10^{-9}
1.0	0.323847486	4.1×10^{-9}	– 0.721231559	1.5×10^{-10}
1.5	0.238385132	2.9×10^{-9}	– 0.579104152	7.4×10^{-9}
2.0	0.174432548	2.7×10^{-9}	– 0.469128657	3.1×10^{-9}
2.5	0.129173356	6.0×10^{-9}	– 0.387902676	1.1×10^{-8}
3.0	0.097565091	7.5×10^{-8}	– 0.328027751	8.9×10^{-9}
3.5	0.075327395	4.2×10^{-8}	– 0.283104721	4.9×10^{-8}
4.0	0.059421371	3.3×10^{-8}	– 0.248573646	5.6×10^{-9}
4.5	0.047814812	1.4×10^{-10}	– 0.221370695	7.7×10^{-10}
5.0	0.039169621	3.0×10^{-9}	– 0.199455354	5.7×10^{-9}

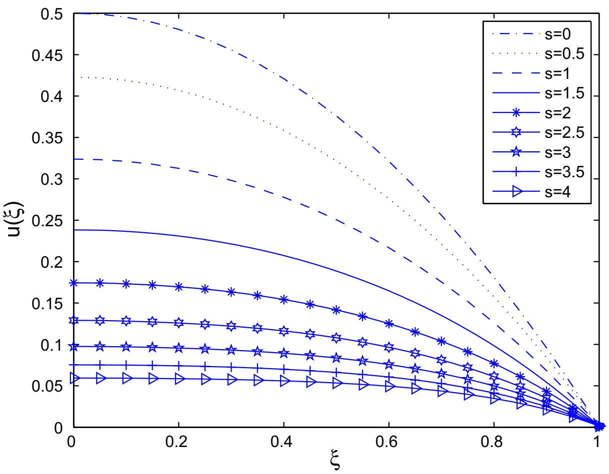

Fig. 2 Plot of $u(\xi)$, when the porous media shaped parameter s is varying and $F = m = 1$

the initial conditions. Then, it applies the Runge–Kutta method to solve the resultant ODE. Also, this range of errors are valid in finding $u'(1)$. In Fig. 2, the plot of $u(\xi)$ is shown, when $F = m = 1$, and porous media shaped parameter s is varying. Increasing the porous media shaped parameter causes the decreasing behavior of $u(\xi)$. We have to notify that in the third step of $SL_2(R)$-shooting method algorithm if $s \to \infty$ then $\varpi \to \infty$. Hence, both of $\theta_1^0(n)$ and $\theta_2^f(n)$ tend to infinity. Therefore, our presented algorithm fails for large values of the parameter s.

Values of $u(0)$ and $u'(1)$ and their absolute errors with different values of Forchheimer number F and $s = m = 1$ are presented in Table 2. The range of absolute errors from this table is $10^{-9} \sim 10^{-13}$. In Fig. 3, the plot of $u(\xi)$ is shown, when $m = s = 1$ and Forchheimer number is varying. Also, $u(\xi)$ will decrease when the Forchheimer number is increasing.

Table 2 Obtained values and absolute errors of $u(0)$ and $u'(1)$ with $SL_2(R)$ method, when $s = m = 1$ and F is varying

F	$u(0)$–$SL_2(R)$	Error of $u(0)$	$u'(1)$–$SL_2(R)$	Error of $u'(1)$
1	0.3238474860	4.1×10^{-9}	– 0.7212315596	1.5×10^{-10}
2	0.3026092007	1.8×10^{-10}	– 0.6904336083	4.1×10^{-11}
3	0.2856673470	2.4×10^{-10}	– 0.6656610379	3.8×10^{-13}
4	0.2716687936	9.0×10^{-10}	– 0.6450320806	1.1×10^{-10}
5	0.2598041355	4.7×10^{-11}	– 0.6274198915	7.4×10^{-11}
6	0.2495532690	7.8×10^{-10}	– 0.6120981575	9.4×10^{-12}
7	0.2405624459	2.0×10^{-12}	– 0.5985716174	1.1×10^{-10}
8	0.2325805720	1.8×10^{-11}	– 0.5864878180	1.8×10^{-11}
9	0.2254232465	5.1×10^{-10}	– 0.5755872580	1.4×10^{-9}
10	0.2189512154	3.5×10^{-11}	– 0.5656735108	2.3×10^{-11}

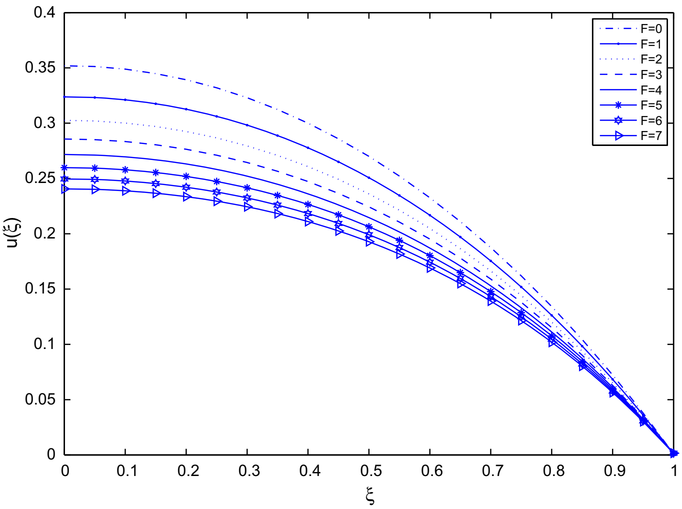

Fig. 3 Plot of $u(\xi)$, when the Forchheimer parameter F is varying and $s = m = 1$

Now, to demonstrate the dependence of the solution to the viscosity ratio (m), we plot the solution when it is varying and $F = s = 1$, Fig. 4. In Table 3, we show the values of $u(0)$, $u'(1)$, and their related absolute errors, obtained by $SL_2(R)$-shooting method.

To illustrate the efficiency and power of the current method, we take into account the case $F = 0$, of which this assumption leads to the exact solution of Eq. (1.1) as:

$$u(\xi) = \frac{1}{ms^2} + c_1 e^{s\xi} + c_2 e^{-s\xi}, \tag{4.47}$$

and imposing the boundary conditions $u(1) = 0$ and $u'(0) = 0$ yields:

$$u(\xi) = \frac{1 + e^{2s} - e^{s(1-\xi)} - e^{s(1+\xi)}}{ms^2(1 + e^{2s})}. \tag{4.48}$$

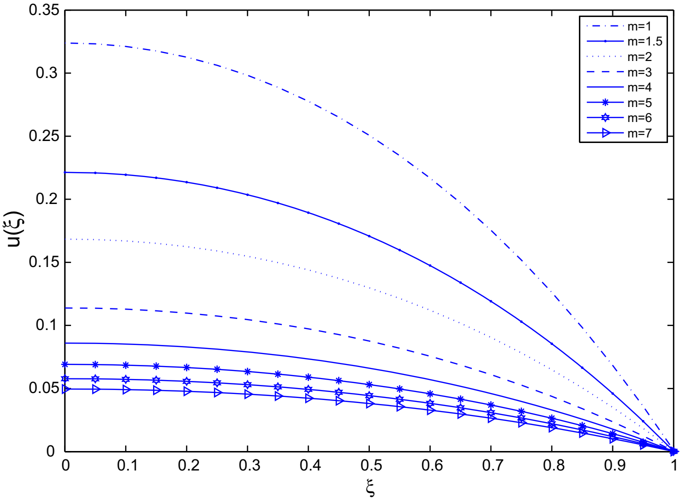

Fig. 4 Plot of $u(\xi)$, when the viscosity ratio m is varying and $s = F = 1$

Table 3 Obtained values and absolute errors of $u(0)$ and $u'(1)$ with $SL_2(R)$ method, when $s = F = 1$ and m is varying

m	$u(0)$–$SL_2(R)$	Error of $u(0)$	$u'(1)$–$SL_2(R)$	Error of $u'(1)$
1	0.3238474860	4.1×10^{-9}	− 0.7212315596	1.5×10^{-10}
2	0.1684008977	1.5×10^{-10}	− 0.3699435949	1.6×10^{-10}
3	0.1138578083	2.8×10^{-10}	− 0.2489128381	1.1×10^{-9}
4	0.0860143800	6.9×10^{-10}	− 0.1875752290	1.0×10^{-10}
5	0.0691162781	2.1×10^{-10}	− 0.1504969649	7.4×10^{-10}
6	0.0577686157	8.7×10^{-10}	− 0.1256601313	1.0×10^{-9}
7	0.0496221220	5.8×10^{-11}	− 0.1078607239	8.9×10^{-10}
8	0.0434895302	7.8×10^{-11}	− 0.0944786081	1.4×10^{-9}
9	0.0387061424	2.0×10^{-10}	− 0.0840508229	5.1×10^{-10}
10	0.0348708046	4.9×10^{-10}	− 0.0756962349	7.0×10^{-10}

Note that from Eq. (4.48), we have:

$$u(0) = \frac{(\mathrm{e}^{s} - 1)^2}{ms^2(1 + \mathrm{e}^{2s})}. \tag{4.49}$$

In Fig. 5, the absolute errors of approximated solutions with the initial condition (4.49) and different values of porous media shaped parameter and viscosity ratio are plotted. It is remarkable that the errors are in the order 10^{-8}. Finally, in Tables 4 and 5, we obtained the solution $u(\xi)$ with RKHS method with respect to some various parameters and $n = 1000$. Then, we compared the obtained approximate solutions with the results of $SL_2(R)$-shooting method. Closed results of these two methods show the confidence of applied methods.

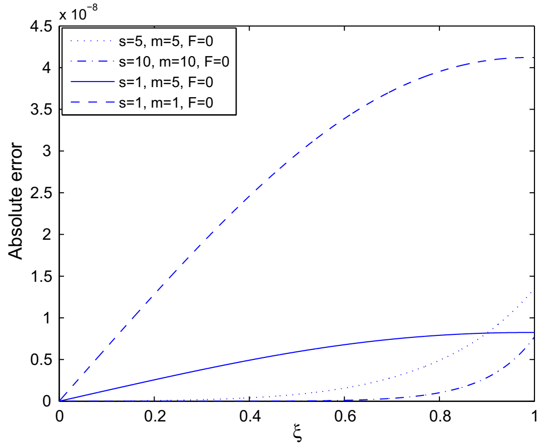

Fig. 5 Absolute errors with respect to different values of m and s when $F = 0$

Table 4 Obtained solutions $u(\xi)$ with respect to $s = F = m = 1$

ξ	RKHS	$SL_2(R)$
0.0	0.3238451032	0.3238474860
0.1	0.3209962563	0.3209904454
0.2	0.3123621102	0.3123456455
0.3	0.2978204245	0.2978275245
0.4	0.2771497852	0.2771989887
0.5	0.2500031045	0.2507802349
0.6	0.2159745124	0.2198854472
0.7	0.1745685674	0.1744523456
0.8	0.1252068582	0.1252645237
0.9	0.0672431142	0.0672430522
1.0	0.0	0.0

Table 5 Obtained solutions $u(\xi)$ with respect to $s = 1,\ F = 2$, and $m = 3$

ξ	RKHS	$SL_2(R)$
0.0	0.1107570712	0.1107570712
0.1	0.1097656541	0.1097657230
0.2	0.1067702559	0.1067772980
0.3	0.1017497845	0.1017488328
0.4	0.0946090456	0.0946093015
0.5	0.0852569241	0.0852593143
0.6	0.0735796532	0.0735716975
0.7	0.05939202113	0.0593925930
0.8	0.0425426662	0.0425426618
0.9	0.0228193469	0.0228193209
1.0	0.0	0.0

5 Conclusions

In this study, we explored two powerful methods for solving the nonlinearity arising from forced convection in a porous-saturated duct. First, we discussed a geometric method, namely $SL_2(R)$-shooting method, which is based on the Lie groups. We proposed a simple algorithm to find the approximate solution of the current model. The figures and tables clearly demonstrate that $SL_2(R)$-shooting method provides excellent results to the solution of the current model with high accuracy. Then, we investigated the solution of the model by a mesh-free method, namely RKHS method. Convergence analysis of this method was theoretically considered, and finally, a comparison of the obtained solutions with both of the proposed methods shows that the results are very closed and confident. It is remarkable that by the same stepsizes, the $SL_2(R)$ method gives more accurate solutions than the RKHS method. However, it is obvious that if we increase the number of iterations or number of collocation points, we can get very closed results by the RKHS method.

Acknowledgements The authors would like to thank the referees for useful comments and remarks.

Compliance with ethical standards

Conflict of interest The authors declare no conflict of interest.

References

1. C.-S. Liu, Cone of non-linear dynamical system and group preserving schemes. Int. J. NonLinear Mech. **36**, 1047–1068 (2001)
2. M.S. Hashemi, D. Baleanu, M. Parto-Haghighi, E. Darvishi, Solving the time-fractional diffusion equation using a Lie group integrator. Thermal Sci. **19**, 77–83 (2015)
3. M.S. Hashemi, E. Darvishi, D. Baleanu, A geometric approach for solving the density-dependent diffusion Nagumo equation. Adv. Differ. Equ. **2016**, 1–13 (2016)
4. M.S. Hashemi, S. Abbasbandy, A geometric approach for solving Troesch's problem. B. Malays. Math. Sci. Soc. **40**(1), 97–116 (2017)
5. M.S. Hashemi, Constructing a new geometric numerical integration method to the nonlinear heat transfer equations. Commun. Nonlinear Sci. Numer. Simul. **22**, 990–1001 (2015)
6. S. Abbasbandy, M.S. Hashemi, C.-S. Liu, The Lie-group shooting method for solving the Bratu equation. Commun. Nonlinear Sci. Numer. Simul. **16**, 4238–4249 (2011)
7. S. Abbasbandy, M.S. Hashemi, Group preserving scheme for the Cauchy problem of the Laplace equation. Eng. Anal. Bound. Elem. **35**, 1003–1009 (2001)
8. M.S. Hashemi, A novel simple algorithm for solving the magneto-hemodynamic flow in a semi-porous channel. Eur. J. Mech. B/Fluids **65**, 359–367 (2017)
9. M.S. Hashemi, M. Inc, E. Karatas, A. Akgül, A numerical investigation on Burgers equation by mol-gps method. J. Adv. Phys. **6**(3), 413–417 (2017)
10. A. Akgül, M.S. Hashemi et al., Group preserving scheme and reproducing kernel method for the Poisson–Boltzmann equation for semiconductor devices. Nonlinear Dyn. **88**(4), 2817–2829 (2017)
11. A. Akgül, M.S. Hashemi, S. Raheem et al., Constructing two powerful methods to solve the Thomas–Fermi equation. Nonlinear Dyn. **87**(2), 1435–1444 (2017)
12. N. Shawagfeh, O.Abu Arqub, S. Momani, Analytical solution of nonlinear second-order periodic boundary value problem using reproducing kernel method. J. Comput. Anal. Appl. **16**(4), 750–762 (2014)
13. O.A. Arqub, The reproducing kernel algorithm for handling differential algebraic systems of ordinary differential equations. Math. Methods Appl. Sci. **39**(15), 4549–4562 (2016)
14. O.A. Arqub, M. Al-Smadi, N. Shawagfeh, Solving fredholm integro-differential equations using reproducing kernel Hilbert space method. Appl. Math. Comput. **219**(17), 8938–8948 (2013)
15. O.A. Arqub, B. Maayah, Solutions of Bagley–Torvik and Painlevé equations of fractional order using iterative reproducing kernel algorithm with error estimates. Neural Comput. Appl. **29**(5), 1465–1479 (2018)

16. S. Abbasbandy, B. Azarnavid, Some error estimates for the reproducing kernel Hilbert spaces method. J. Comput. Appl. Math. **296**, 789–797 (2016)
17. S. Abbasbandy, B. Azarnavid, M.S. Alhuthali, A shooting reproducing kernel Hilbert space method for multiple solutions of nonlinear boundary value problems. J. Comput. Appl. Math. **279**, 293–305 (2015)
18. P. Bakhtiari, S. Abbasbandy, R.A. Van Gorder, Solving the dym initial value problem in reproducing kernel space. Numer. Algorithms **78**, 1–17 (2018)
19. M. Awartani, M. Hamdan, Fully developed flow through a porous channel bounded by flat plates. Appl. Math. Comput. **169**(2), 749–757 (2005)
20. K. Hooman, A perturbation solution for forced convection in a porous-saturated duct. J. Comput. Appl. Math. **211**(1), 57–66 (2008)
21. S. Abbasbandy, E. Shivanian, I. Hashim, Exact analytical solution of forced convection in a porous-saturated duct. Commun. Nonlinear Sci. Numer. Simul. **16**(10), 3981–3989 (2011)